

# Evolution of Abundances and spectra in the large solar energetic particle events of 1998 Sep 30 and 2000 Apr 4

C. K. Ng<sup>1,3</sup>, D. V. Reames<sup>1</sup>, and A. J. Tylka<sup>2</sup>

<sup>1</sup>Laboratory for High Energy Astrophysics, NASA Goddard Space Flight Center, Greenbelt, MD 20771, USA

<sup>2</sup>E. O. Hulburt Center for Space Research, Naval Research Laboratory, Washington, DC 20375, USA

<sup>3</sup>Department of Astronomy, University of Maryland, College Park, MD 20742, USA

**Abstract.** The 1998 Sep 30 and 2000 Apr 4 events are both large western solar energetic particle (SEP) events, in which  $\sim 1$  MeV proton intensities exceed  $10^3$  particles  $(\text{cm}^2 \text{ s sr MeV})^{-1}$ . Yet they exhibit quite different time variations of elemental abundance ratios and energy spectra. Using a model of SEP transport through self-amplified interplanetary Alfvén waves, we fit the simultaneous observations of protons and ions of helium, oxygen, and iron. We conclude that wave amplification by high energy protons largely account for the differences in the observed time histories.

anisotropy variations between large and small events (Reames et al., 2000, 2001). More precisely, large streaming of  $> 10$  MeV protons is required for wave amplification to affect the transport of  $\sim$  MeV/amu ions. Thus, the 1998 Sep 30 and 2000 Apr 4 events are especially interesting in that their peak proton intensities are both large at 1 MeV, but the latter's is smaller by a factor of  $\sim 40$  at 20 MeV. In this paper, we apply a model of the coupled evolution of SEPs and IP Alfvén waves to study the different time variations in the H, He, O and Fe spectra, and H/He and Fe/O ratios at a few MeV/amu in these two events, with the aim of assessing the role of wave amplification and other processes.

## 1 Introduction

Wave-particle interaction has provided a foundation for understanding the transport and acceleration of energetic charged particles in astrophysical plasmas, from flaring loops on the sun to the interstellar media. The quasilinear theory has long been used to deduce from interplanetary (IP) magnetic power spectra the particle diffusion coefficients governing the transport of solar energetic particles (SEPs) and cosmic rays in the heliosphere. Since the theory demands that wave amplification go hand in hand with particle scattering, we have explored the role of particle driven waves with a simple model of SEP transport coupled to IP Alfvén waves. We found that particle transport through self-amplified waves accounts semi-quantitatively for the complex yet remarkably systematic and rigidity-dependent evolution of SEP abundances in the 1998 April 20 event (Tylka et al., 1999; Ng et al., 1999a,b). Tylka et al. (2000) suggested it also played an important role in the evolution of particle spectra in that and the 1998 Aug 25 event.

If proton-driven wave growth is important, its effect on abundance variation and anisotropies must increase with proton streaming. This expectation is supported by a comparison of the initial time dependence of SEP abundances and

## 2 Description of Events

**1998 Sep 30.** The intensities of  $\sim 2.2$  MeV protons and helium ions, and  $\sim 3.7$  MeV/amu oxygen and iron ions measured by Wind/LEMT rose rapidly to large values (Fig.1, top). The He/H ratio at  $\sim 2.2$  MeV/amu rose from below coronal values for 6 hrs, then decayed. In contrast, Fe/O at  $\sim 3.7$  MeV/amu started well above coronal values and apart from a soft shoulder, decayed for  $\sim 30$  hours (Fig.1, bottom). In Fig. 3, H, He, O and Fe spectra from 500 keV/amu to 500 MeV/amu, compiled with data from Wind/EPACT/LEMT, ACE/SIS, IMP8/GME, ACE/EPAM, ACE/ULEIS are shown for three epochs. The associated W81 flare occurred at 1402 UT on Sep 30. A shock arrived amidst intensity decay at  $\sim 0700$  UT on Oct 2 (transit time  $\sim 42$ h).

**2000 Apr 4.** The 2.2 MeV H and He intensities rose more slowly than in the Sep 30 event to comparable magnitudes, but O and Fe intensities were much smaller (Fig. 2, top). In contrast to the Sep 30 event, Fe/O and He/H ratios *both* decayed rapidly from large values and Fig. 4 showed much softer particle spectra at 3 epochs. The associated W66 flare occurred at 1511 UT Apr 4, and LASCO observed a CME with a speed of  $\sim 1500$  km/s (M. Andrews, private communication). The particle intensities increased moderately around shock crossing at 1620 UT Apr 6 (transit time also

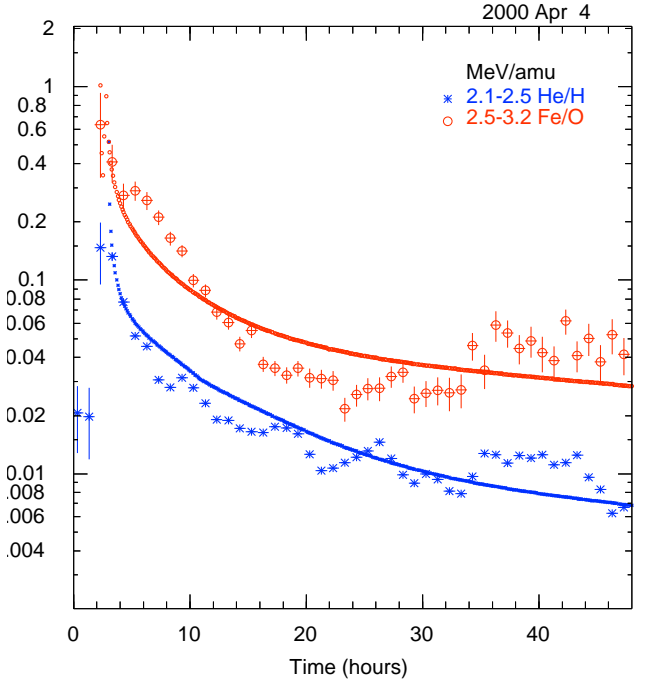
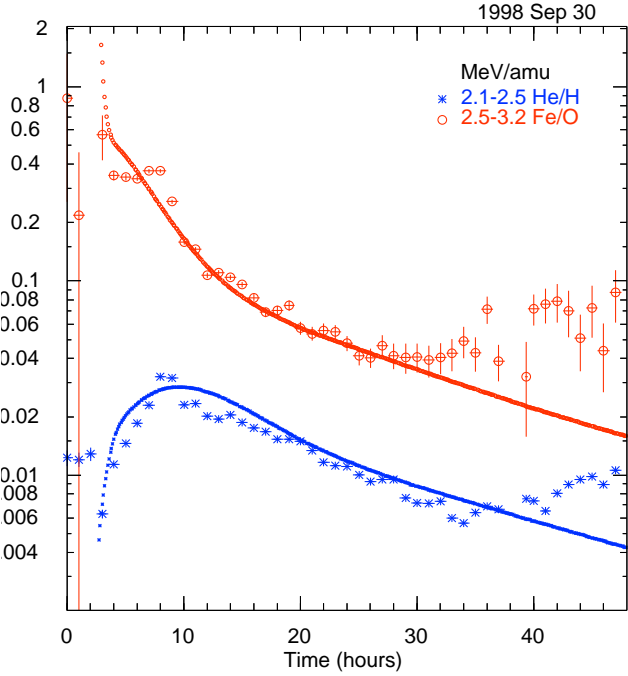
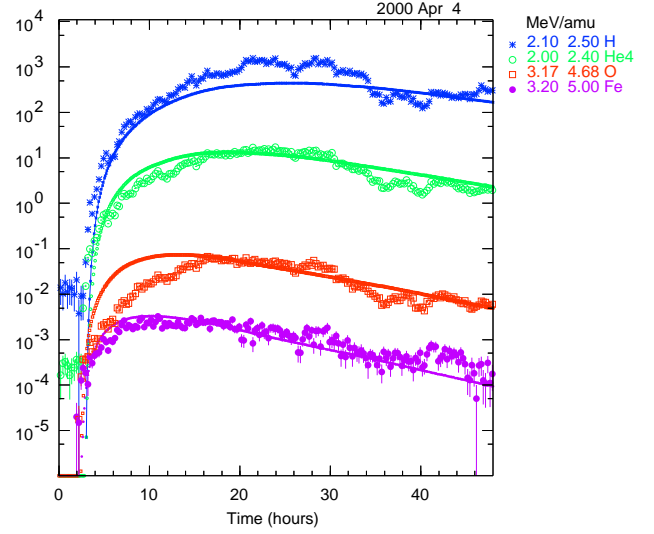
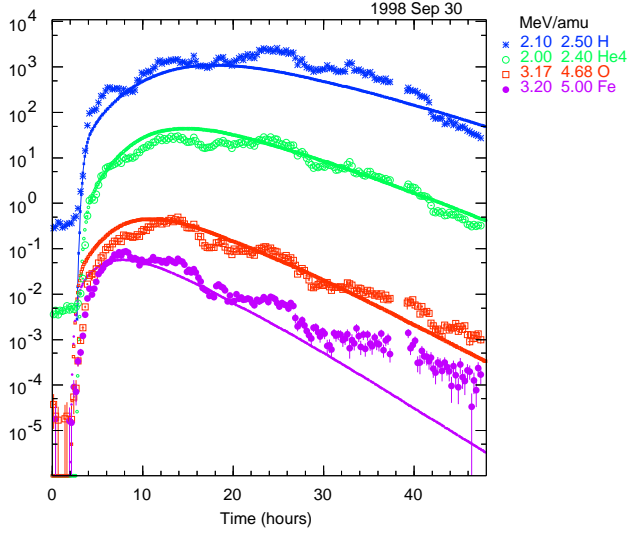


**Fig. 1.** Top: Symbols are Wind/LEMT observed H, He, O, and Fe intensities. Bottom: Fe/O and He/H ratios. Curves: See Fig. 2 caption. 1998 Sep 30 1430 UT is  $t=0$ .

**Fig. 2.** As in Fig.1, for the 2000 Apr 4 event. Curves are model predictions using ion source with O/H, Fe/H, He/H of 1, 1,  $0.5\times$  coronal values. 2000 Apr 4 1511 UT is  $t=0$ .

$\sim 42$ h).

### 3 Model

SEPs are injected at a shock traveling through the solar wind plasma with an initial distribution of Alfvén waves. The evolution of the phase-space densities  $f_s(\mu, P, r, t)$  of ion species  $s$  and the spectral density  $I_\sigma(k, r, t)$  of  $\sigma$ -mode Alfvén waves are coupled via quasilinear theory. The model includes, for particles: magnetic focusing, quasilinear pitch-angle scattering by waves, solar-wind convection, and adiabatic deceleration; and for waves: quasilinear interaction

with SEPs, kinetic transport in the solar wind, and phenomenological damping of waves. For simplicity we assume a radial magnetic field, and constant solar wind and shock velocities. The basic features of the model have been described in Ng et al.(1999b). The governing equations are given below in “mixed coordinates”:  $(r, t)$  in fixed inertial frame and  $(\mu, P)$  in the solar-wind frame,

$$\frac{\partial F_s}{\partial t} + \frac{\partial}{\partial r}[(\mu v + W)F_s] + \frac{\partial}{\partial \mu} \left[ \frac{1 - \mu^2}{r} (v + \mu W) F_s \right] - P \frac{\partial}{\partial P} \left[ \frac{1 - \mu^2}{r} W F_s \right] - \frac{\partial}{\partial \mu} \left[ D_{\mu\mu}^s \frac{\partial F_s}{\partial \mu} \right] = G_s \quad (1)$$

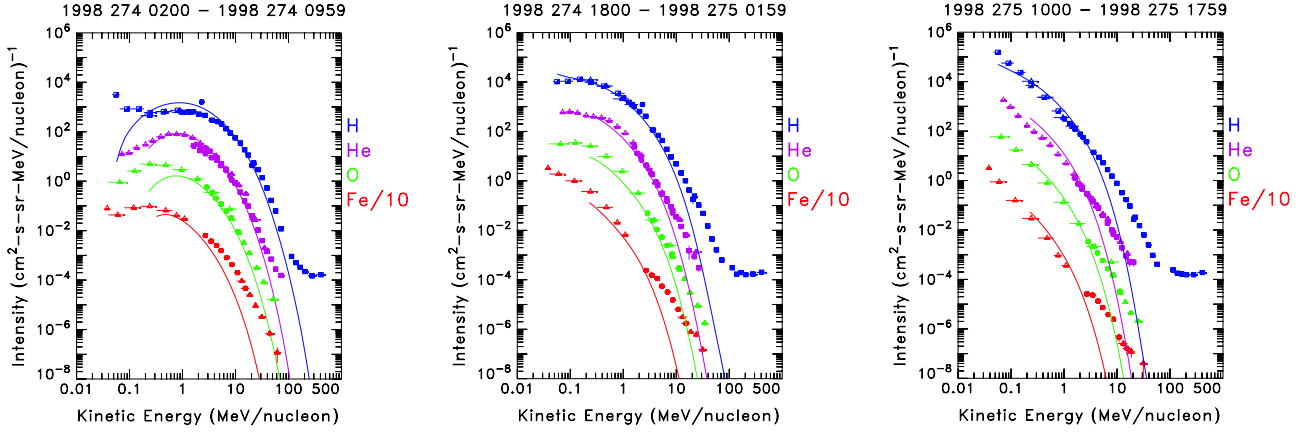


**Fig. 3.** Spectra of H, He, O, and Fe in the 1998 Sep 30 Event at 3 epochs, centered at 17, 33, and 48 hours after onset. Data are compiled from Wind/EPACT/LEMT (filled circles), ACE/SIS (filled triangles), IMP8/GME (filled squares), ACE/EPAM (half-filled squares), ACE/ULEIS (half-filled triangles). The curves are computed from the model.

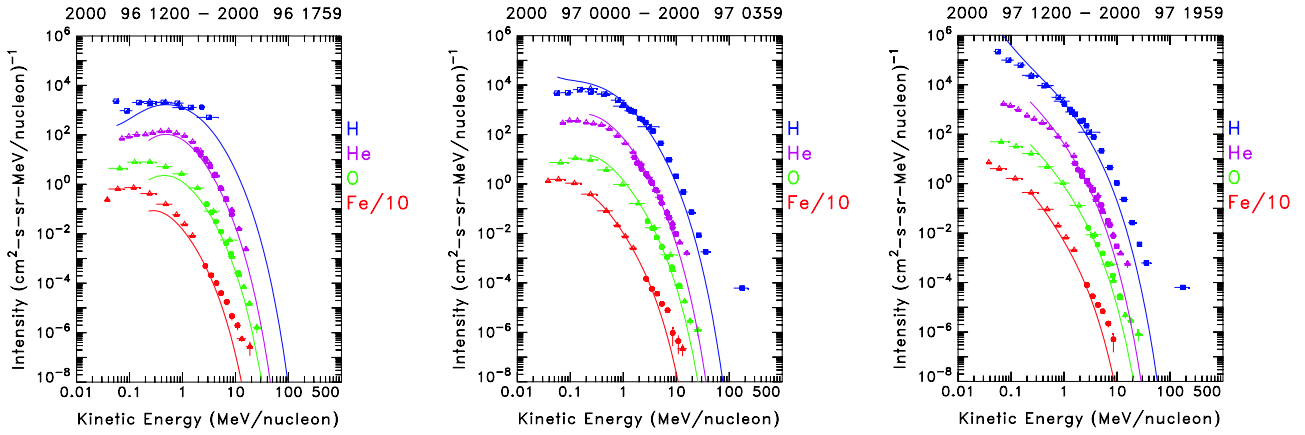


**Fig. 4.** As in Fig.3, for the 2000 Apr 4 event at 23, 34, and 47 hours after onset. IMP8 H and He data gap in panel 1.

$$\frac{\partial \Psi_\sigma}{\partial t} + \frac{\partial}{\partial r} (V_\sigma \Psi_\sigma) + \frac{\partial}{\partial \eta} \left[ \left( 2 \frac{V_\sigma}{r} - \frac{dV_\sigma}{dr} \right) \Psi_\sigma \right] = \gamma_\sigma \Psi_\sigma \quad (2)$$

$$D_{\mu\mu}^s = \frac{v^2}{4P^2} \sum_\sigma \int dk I_\sigma(k, r, t) R_{\mu\mu}^\sigma(\mu, v, P, k, V_\sigma) \quad (3)$$

$$\gamma_\sigma = 2\pi^2 g_\sigma e^3 c V_A \iint d\mu dP \frac{P^3}{E^2} \frac{R_{\mu\mu}^\sigma}{(1 - \mu V_\sigma/v)^2} \frac{\partial f_H}{\partial \mu} + \zeta_1 + \zeta_2 (k/B)^\beta [I_\sigma(k, r, t)/I_\sigma(k, r, 0) - 1] \quad (4)$$

$$F_s(\mu, P, r, t) = f_s(\mu, P, r, t) (B_0 P^3) / (B P_{0,s}^3) \quad (5)$$

$$\Psi_\sigma(k, r, t) = 2I_\sigma(k, r, t) (k B_0 V_\sigma) / (k_0 B V_A) \quad (6)$$

In the above,  $t$  is time,  $r$  heliocentric distance,  $v$  ion velocity,  $P$  rigidity,  $\mu$  pitch-angle cosine,  $D_{\mu\mu}^s(P, \mu, r, t)$  species- $s$  diffusion coefficient in  $\mu$ -space,  $B = B_0(r_0/r)^2$  magnetic field,  $k$  wavenumber,  $\eta = \ln(k/B)$ ,  $G_s$  ion source term,  $\gamma_\sigma$  growth rate of  $I_\sigma$ ,  $c$  light speed,  $e$  elementary charge,  $E$  proton total energy,  $V_A = V_{A,0} r_0/r$  Alfvén speed,  $W$  solar-wind speed,  $V_{sh}$  shock speed,  $r_{sh} = r_{0,sh} + tV_{sh}$  shock distance from Sun,  $g_\sigma = \pm 1$  for outward (inward) waves,  $V_\sigma = W + g_\sigma V_A$ ,  $B_0$ ,  $k_0$ ,  $r_0$  and  $r_{0,sh}$  are constants, and  $R_{\mu\mu}^\sigma(\mu, v, P, k, V_\sigma)$  is the wave-particle resonance function (Ng & Reames, 1995).

In eq. (4) only  $f_H$  appears, assuming minor ions contribute negligibly to wave evolution (Lee, 1983). The parameters  $\zeta_1 < 0$  and  $\zeta_2 < 0$  specify ad hoc damping rates on the ambient and amplified waves, respectively, and  $\beta$  controls the latter's dependence on  $k/B$ . The isotropic ion source  $G_s$  per  $(\text{cm}^2 \text{ MV}^3 \text{ h})$  in eq. (1) is localized at the shock within  $\pm \Delta r/2$ , with  $\Delta r = 0.0125$  AU the computational spatial grid size, such that

$$\int_{r_{sh}-\Delta r/2}^{r_{sh}+\Delta r/2} G_s dr = \frac{(\delta-3) b n_{s,0} (V_{sh} - W)}{4\pi P_{0,s}^3} \times \left( \frac{P}{P_{0,s}} \right)^{3-\delta} \exp \left[ \frac{-(r_{sh} - r_{0,sh})}{r_d} \right] \exp \left( \frac{-e v P}{2c E_{kn}} \right). \quad (7)$$

The spectral index  $\delta = \delta_0 + \delta' V_{sh} t$  is assumed identical for all species.  $b \ll 1$  is the maximum seed-particle fraction of the solar wind flux into the shock,  $n_{s,0} r_0^2/r^2$  the solar-wind  $s$ -ion density at  $r$  with  $r_0 \equiv 1$  AU,  $P_{0,s}$  the “seed” ion rigidity,  $r_d$  the source decay length, and  $E_{kn} = E_{0,kn}(r_{0,sh}/r_{sh})$  the exponential rollover energy (cf. the radial dependence of maximum energy in Zank et al. (2000)). These parameters allow us to study the effects of various temporal, spatial, and

spectral characteristics of the shock-accelerated ion source.

For the simulation, we start with empty ion distributions and outward propagating Alfvén wave distributions which are steady-state solutions of eq.(2), with power-law spectral index  $\alpha$  and wave intensity  $I_{00}$  at  $r=1$  AU and  $k/B = 2.308 \times 10^{-2} \text{ MV}^{-1}$ . The coupled equations are solved by finite-difference technique (Ng & Reames, 1994).

#### 4 Comparison of theory with observation

We performed a large number of computer runs with the model. For each of the observed events, we select the results of one run to display as curves superposed on the observed data on the intensity, abundance ratio, and spectra (Figs. 1-4). These are not best fits, but our preliminary attempts to compare theory and observation. We obtain reasonably good fit to all observed histories of intensities and abundance ratios in Figs.1 and 2, except for the slow rise in the observed oxygen intensity in the Apr 4 event. The calculated spectra fit the observations on the whole, but are softer than observed at high energies, implying that we could do better with slightly harder source spectra. We emphasize that the model predicts absolute intensities for all species; the particle sources have been specified with identical energy spectral shapes, and the O/H, Fe/H, and He/H ratios in the source are set to 1, 1, and  $0.5 \times$  the known coronal values (Reames, 1999). The proton intensity at high energies critically determines the amplified level of Alfvén waves that scatter  $\sim \text{MeV}/\text{amu}$  ions.

The following parameters are common for both event fits:  $n_{\text{H},0} = 5 \text{ cm}^{-3}$ ,  $P_{0,\text{H}} = 3.06 \text{ MV}$ ,  $r_{0,\text{sh}} = 0.1125 \text{ AU}$ ,  $V_{\text{sh}} = 0.024 \text{ AU h}^{-1}$ ,  $V_{\text{A},0} = 0.001 \text{ AU h}^{-1}$ ,  $\alpha = -1.7$ ,  $\zeta_2 = -0.30 \text{ h}^{-1}$ , and oxygen and iron charge states of 6.67 and 11.67, respectively.

For the 1998 Sep 30 event, the other model parameters are:  $b = 0.003$ ,  $\delta_0 = -4$ ,  $E_{0,\text{kn}} = 80 \text{ MeV}$ ,  $\delta' = -3 \text{ AU}^{-1}$ ,  $r_d = 0.2 \text{ AU}$ ,  $\zeta_1 = -0.012 \text{ h}^{-1}$ ,  $I_{00} = 2.5 \times 10^3 \text{ MeV cm}^{-2}$ ,  $\beta = 0.25$ , and  $W = 0.011 \text{ AU h}^{-1}$ . For the 2000 Apr 4 events, these are:  $b = 0.1$ ,  $\delta_0 = -5.5$ ,  $E_{0,\text{kn}} = 10 \text{ MeV}$ ,  $\delta' = -2 \text{ AU}^{-1}$ ,  $r_d = \infty$ ,  $\zeta_1 = -0.011 \text{ h}^{-1}$ ,  $I_{00} = 1 \times 10^4 \text{ MeV cm}^{-2}$ ,  $\beta = 1$ , and  $W = 0.01 \text{ AU h}^{-1}$ .

For the 2000 Apr 4 event, the initial wave intensities are set higher to fit the slower intensity rise; the source spectral index  $\delta_0 = -5.5$  and the e-folding “knee” energy  $E_{0,\text{kn}} = 10 \text{ MeV}$  result from the observed soft spectra. The observed large proton intensity below  $\sim 1 \text{ MeV}$  then leads to  $b=0.1$ , i.e.  $\sim 10\%$  of the solar wind flux is accelerated by the shock, *if* the source spectra extend down to  $5 \text{ keV}/\text{amu}$ . Obviously, the source spectra must flatten below  $500 \text{ keV}/\text{amu}$ , the lowest energy in the spectra reported here. By contrast,  $b=0.003$  for the 1998 Sep 30 event is quite reasonable.

Our computations indicate that for the 1998 Sep 30 event with large intensities at  $> 10 \text{ MeV}$ , unmitigated proton-driven wave growth modifies particle intensities more severely than observed. Hence we introduced phenomenological wave damping in eq. (4) to moderate wave growth and bring the computed intensities closer to the observation. The fit parameters for damping in the two events are not significantly differ-

ent. In both events, the calculated spectra are softer than observed at high energies, and the fits could improve with harder source spectra. The observed iron spectra become harder than other species at high energies. Tylka et al. (2001 ICRC) attribute similar features in the 2000 July 14 event to the shock acceleration of highly ionized iron superthermal left over from previous impulsive events.

#### 5 Conclusion

On the whole, the model predictions agree well with the observed evolution of the spectra and intensity of all ion species and the He/H and Fe/O ratios. Given the wide range of energies and particle species, this overall agreement is encouraging, especially since the source abundances are chosen close to the observed coronal composition. The success of the model in reproducing the contrasting behavior of hard and soft SEP events with high  $\sim \text{MeV}$  proton intensities corroborates the findings in our previous studies contrasting large and small SEP events (Reames et al., 2000, 2001), and lends further support to the role of proton generated waves.

*Acknowledgements.* ACE Level 2 data were provided by the ACE website at <http://www.srl.caltech.edu/ACE/>. AJT was supported by the ACE Guest Investigator Program under NASA DPR W19,501.

#### References

- Lee, M.A. 1983, JGR 88, 6109
- Ng, C.K. & Reames, D. V. 1994, ApJ 424, 1032
- Ng, C.K. & Reames, D.V. 1995, ApJ 453, 890
- Ng, C.K., Reames, D.V., & Tylka, A.J. 1999a, GRL 26, 2145
- Ng, C.K., Reames, D.V., & Tylka, A.J. 1999b, Proc. 26th ICRC (Salt Lake City), 6, 151
- Reames, D.V. 1999, Space Sci. Rev. 90, 413
- Reames, D.V., Ng, C.K., & Tylka, A.J. 2000, ApJ 531, L83
- Reames, D.V., Ng, C.K., & Berdichevsky, D. 2001, ApJ 550, 1064
- Tylka, A.J., Reames, D.V., & Ng, C.K. 1999, GRL 26, 2141
- Tylka, A.J., Boberg, P.R., McGuire, R.E., Ng, C.K., & Reames, D.V. 2000, in AIP Conf. Proc. 528, ed. R.A. Mewaldt et al. (New York: AIP), 147
- Zank, G.P., Rice, W.K.M., & Wu, C.C. 2000, JGR, 105, 25079